Journal of the Korean Association of Geographic Information Studies, 22(1) 2019, pp.129-139 ISSN 1226-9719(Print)On
https://doi.org/10.11108/kagis.2019.22.1.129 ISSN 2287-6952(Online)

A Study on the Evaluation of the Different Thresholds for Detecting Urban Areas Using Remote-Sensing Index Images: A Case Study for Daegu, South Korea*

Yun-Jae CHOUNG[1] · Eung-Joon LEE[2] · Myung-Hee JO[3]※

원격탐사 지수 영상으로부터 도시 지역 탐지를 위한 임계점 평가에 관한 연구: 대구광역시를 사례로*

정윤재[1] · 이응준[2] · 조명희[3]※

ABSTRACT

Mapping urban areas using the earth observation satellites is useful for monitoring urban expansions and measuring urban developments. In this research, the different thresholds for detecting the urban areas separately from the remote-sensing index images (normalized-difference built-up index(NDBI) and urban index(UI) images) generated from the Landsat-8 image acquired in Daegu, South Korea were evaluated through the following steps: (1) the NDBI and UI images were separately generated from the given Landsat-8 image; (2) the different thresholds (-0.4, -0.2, and 0) for detecting the urban areas separately from the NDBI and UI images were evaluated; and (3) the accuracy of each detected urban area was assessed. The experiment results showed that the threshold -0.2 had the best performance for detecting the urban areas from the NDBI image, while the threshold -0.4 had the best performance for detecting the urban areas from the UI image. Some misclassification errors, however, occurred in the areas where the bare soil areas were classified into urban areas or where the high-rise apartments were classified into other areas. In the future research, a robust methodology for detecting urban areas, including the various types of urban features,

2019년 03월 15일 접수 Received on March 15, 2019 / 2019년 03월 26일 수정 Revised on March 26, 2019 / 2019년 03월 26일 심사완료 Accepted on March 26, 2019

* This research was supported by Kyungpook National University Research Fund, 2018.

1 경북대 국토위성정보연구소 Global Landsat Satellite Information Center, Kyungpook National University
2 ㈜지오씨엔아이 GIS 연구소 GIS Research Center, Geo C&I Co., Ltd.
3 경북대 융복합시스템공학부 항공위성시스템전공 Dept, of Aero-Satellite Geo-Informatics Engineering, School of Convergence and Fusion System Engineering, College of Science and Technology, Kyungpook National University
※ Corresponding Author E-mail : mhjo@knu.ac.kr

with less misclassification errors will be proposed using the satellite images. In addition, research on analyzing the pattern of urban expansion will be carried out using the urban areas detected from the multi-temporal satellite images.

KEYWORDS : Urban area, Remote-sensing index, Normalized-difference built-up index, Urban index, Landsat-8 satellite image

요 약

지구관측 위성영상을 활용한 도시지역 매핑 작업은 도시지역의 팽창 및 도시발전의 관측을 위해 매우 중요하다. 본 연구에서는 대구광역시를 촬영한 Landsat-8 위성영상의 분광밴드를 이용하여 제작한 두 원격탐사 지수 영상(정규 건축물 지수(NDBI) 영상 및 도시 지수 (UI) 영상) 으로부터 도시지역을 탐지하기 위한 임계점 평가에 관한 연구를 다음과 같이 진행하였다. 우선, Landsat-8 영상의 분광밴드를 이용하여 NDBI 영상과 UI 영상을 각각 제작한다. 그리고 다양한 임계점 (−0.4, −0.2 및 0)을 NDBI 및 UI 영상에 적용하여 도시지역을 탐지하고, 탐지된 도시지역의 정확도를 산출한다. 본 연구를 통해 진행한 실험결과를 분석한 결과, NDBI 영상에서는 임계점으로 -0.2를 적용시켰을 때 탐지된 도시지역의 정확도(88%)가 가장 높았고, UI 영상에서는 임계점으로 -0.4를 적용시켰을 때 탐지된 도시지역의 정확도(88%)가 가장 높았다. 또한, 일부 지역에서는 나지가 도시지역으로 오분류 되었으며, 고층 아파트 지역이 비도시 지역으로 오분류 되었다. 추후 연구에서는 위성영상에서 오분류를 줄이고 다양한 도시지역 객체를 추출할 수 있는 개선된 방법을 제안하도록 한다. 또한 다중시기 위성영상에서 탐지된 도시지역을 이용하여 도시 팽창 패턴을 분석하는 추후 연구도 수행할 계획이다.

주요어 : 도시지역, 원격탐사 지수, 정규 건축물 지수, 도시 지수, Landsat-8 위성영상

Introduction

An urban area is defined as “the region surrounding a city” and generally consists of human structures like buildings, houses, roads, railways, and bridges(National Geographic, 2019). Identifying the extent of urban areas is necessary for measuring the urban expansion and for monitoring urban development(Choung and Kim, 2019). The earth observation satellite images are useful for mapping urban areas because they include the spectral information necessary for detecting the extent of urban areas(Kim *et al.*, 2003; Kim *et al.*, 2004; and Kim and Kwon, 2009).

Research on identifying urban areas using the various types of satellite images has been carried out of late. In particular, for mapping the urban areas, Sertel and Akay(2015) utilized a high-resolution satellite image, Corbane *et al.*(2008) and Han *et al.*(2017) utilized both the optical and radar satellite images, and Bhatti and Tripathi(2014), Hu *et al.*(2016), Li *et al.*(2017a) and Li *et al.*(2017b) utilized the Landsat images.

Remote-sensing indices made using the spectral bands of satellite images are useful for detecting significant features like

vegetation and water(Jensen, 2016). The urban index(UI) and normalized-difference built-up index(NDBI) are simple remote-sensing indices widely used for detecting urban areas from satellite images(Li *et al.*, 2017a). Research on determining the appropriate thresholds of each NDBI and UI for detecting the various features of urban areas, however, has not been carried out. In the present research, the different thresholds for detecting the various features of urban areas from the NDBI and UI images generated from the given satellite image were evaluated through the following steps: (1) the NDBI and UI images were generated from the given satellite image; (2) the different thresholds (−0.4, −0.2, 0) for detecting the urban areas from the NDBI and UI images were evaluated; and (3) the accuracy of the urban area separately detected from the NDBI and UI images was assessed.

Data and Study Area

For this research, the urban area of Daegu City in South Korea was selected as the study area because it includes the various urban features, such as industrial factory regions, high-rise apartment regions with high elevations, commercial building and housing regions with low elevations. FIGURE 1 shows the urban area of Daegu City in South Korea.

The given Landsat-8 satellite image acquired in the study area on May 12, 2016, with less cloud coverage, consisted of six spectral bands(blue: 0.45-0.51m; green: 0.53-0.59m; red: 0.64-0.67m; near infrared(NIR): 0.85-0.88m; shortwave infrared 1(SWIR1): 1.57-1.65m; and shortwave infrared 2(SWIR2): 2.11-2.29 □m) with a 15m pan-sharpened spatial resolution(United States Geological Survey (USGS), 2019).

As can be seen in FIGURE 1, the

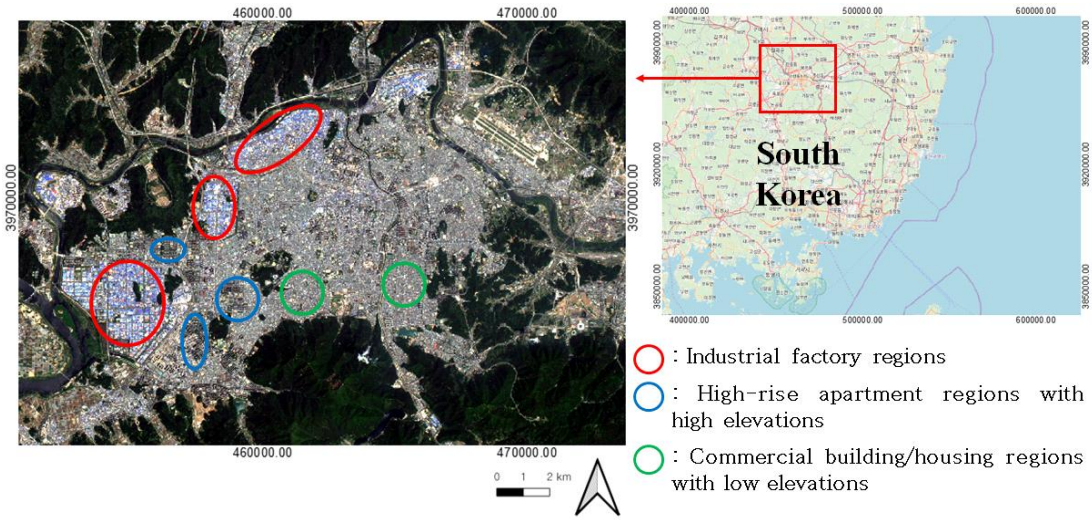

FIGURE 1. Urban area of Daegu City in South Korea, selected as the study area

selected study area includes multiple urban features, such as industrial factory regions, commercial building/housing regions with low elevations, and high-rise apartment regions with high elevations.

Methodology

FIGURE 2 shows the flowchart showing the procedure for evaluating the different thresholds for detecting urban areas from the NDBI and UI images generated from the given Landsat-8 image.

1. Generation of NDBI and UI images

The NDBI image was generated using the equation below(Li *et al.*, 2017a).

$$\frac{SWIR1-NIR}{SWIR1+NIR} \quad (1)$$

where SWIR1 represents shortwave infrared band 1 and NIR represents the near-infrared band of the given Landsat-8 satellite image. The UI image was generated using the equation below(Li et al., 2017a).

$$\frac{SWIR2-NIR}{SWIR2+NIR} \quad (2)$$

where SWIR2 represents shortwave infrared band 2 of the given Landsat-8 satellite image.

FIGURE 3 shows both the NDBI and UI images generated using the SWIR1, SWIR2, and NIR bands of the given Landsat-8 satellite image.

As can be seen in FIGURE 3, the pixels representing the urban areas had high values close to 1 while those representing the other areas had low values close to -1 in both the NDBI and UI images.

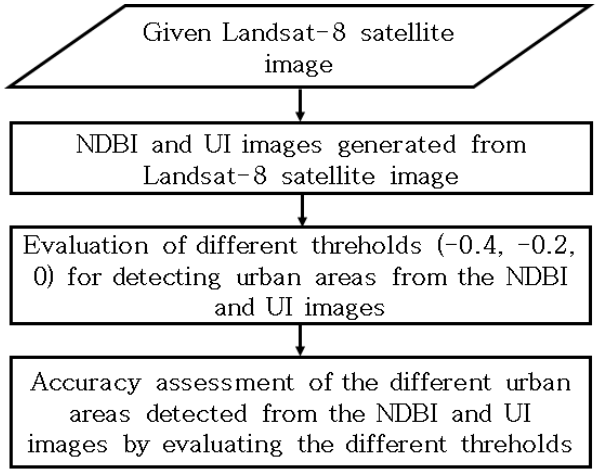

FIGURE 2. Flowchart showing the procedure for evaluating the different thresholds for detecting urban areas from the NDBI and UI images generated from the given Landsat-8 satellite image

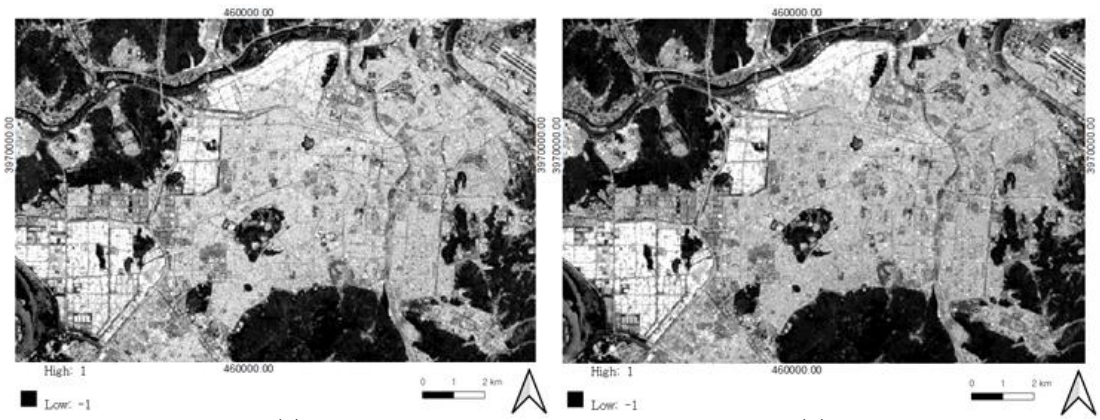

FIGURE 3. NDBI and UI images generated using the SWIR1, SWIR2, and NIR bands of the given Landsat-8 satellite image: (a) NDBI image; and (b) UI image

2. Evaluation of the different thresholds for detecting the urban areas

After both the NDBI and UI images were generated, the different thresholds (−0.4, −0.2, 0) for detecting the urban areas separately from the NDBI and UI images were evaluated. FIGURES 4 and 5 both show the given Landsat-8 satellite image, but FIGURE 4 also shows the urban areas separately detected from the NDBI image by evaluating the different thresholds(−0.4, −0.2, and 0), and FIGURE 5 also shows the urban areas separately detected from the UI image in the same way.

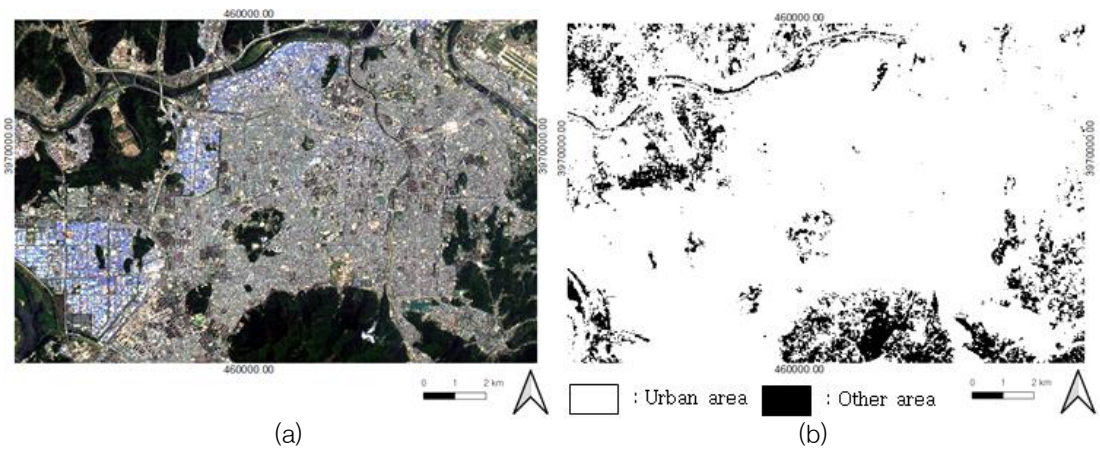

FIGURE 4. Given Landsat-8 satellite image and the urban areas separately detected from the NDBI image by evaluating the different thresholds (−0.4, −0.2, and 0): (a) the given Landsat-8 satellite image; (b) the urban area detected from the NDBI image by evaluating the threshold −0.4; (c) the urban area detected from the NDBI image by evaluating the threshold −0.2; and (d) the urban area detected from the NDBI image by evaluating the threshold 0

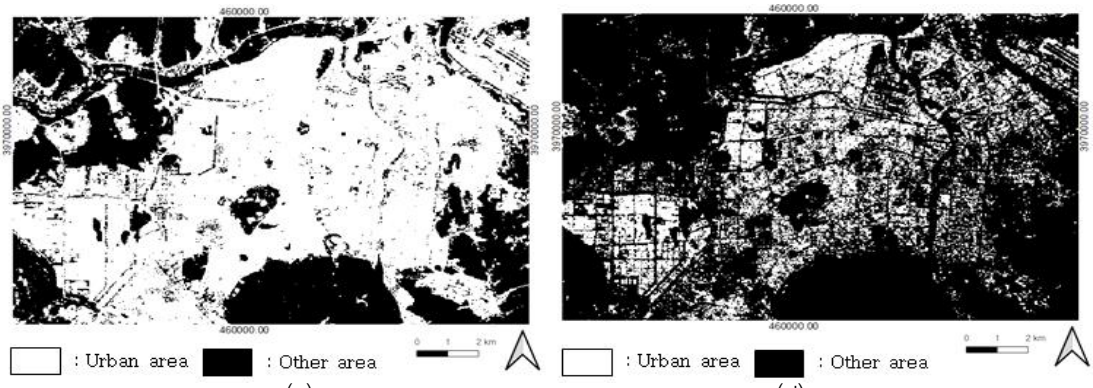

FIGURE 4. Continued

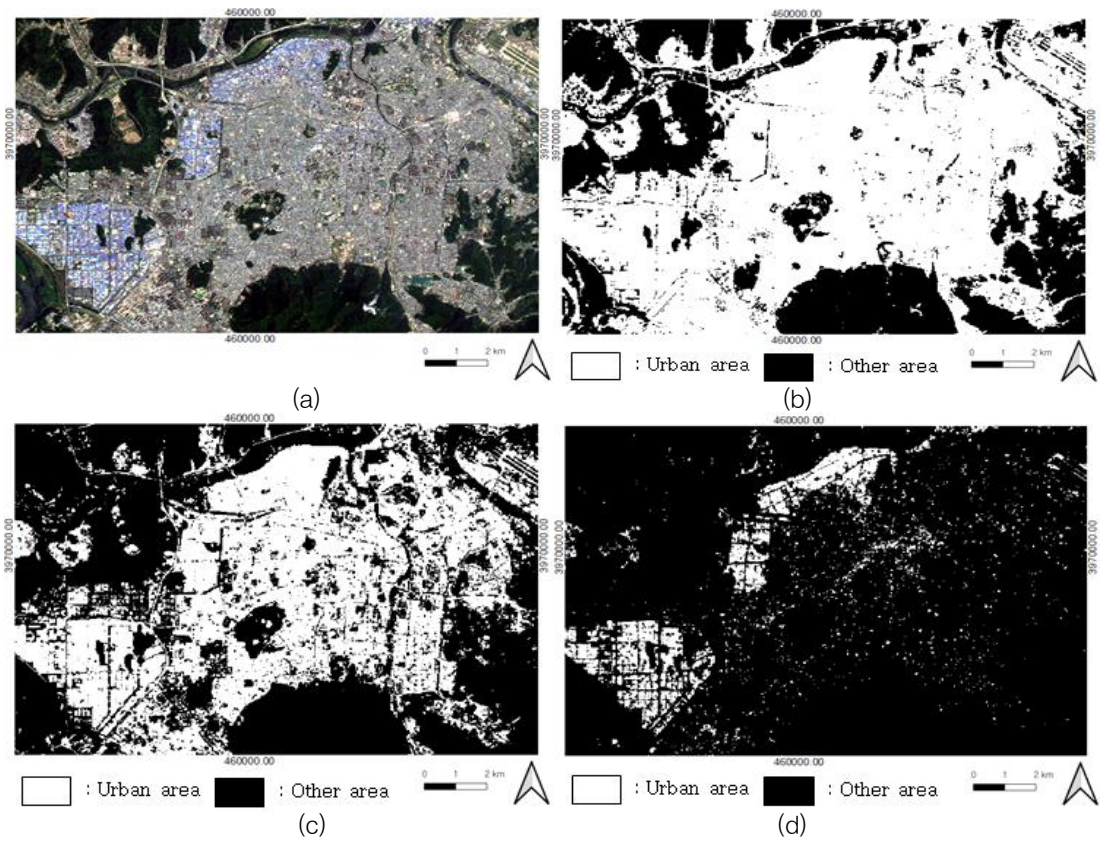

FIGURE 5. Given Landsat-8 satellite image and the urban areas separately detected from the UI image by evaluating the different thresholds (−0.4, −0.2 and 0): (a) the given Landsat-8 satellite image; (b) the urban area detected from the UI image by evaluating the threshold -0.4; (c) the urban area detected from the UI image by evaluating the threshold -0.2; and (d) the urban area detected from the UI image by evaluating the threshold 0

Results and Discussion

1. Measurement of the accuracy of the urban maps

The accuracy levels of all the urban areas separately detected from the NDBI and UI images by evaluating the different thresholds (−0.4, −0.2, and 0) were assessed using the 100 checkpoints manually digitized based on the given Landsat−8 satellite image (see FIGURE 6).

The next step was to assess the overall accuracy of each urban map separately generated from the NDBI and UI images by evaluating the different thresholds. TABLE 1 shows the overall accuracy of each urban map separately generated from the NDBI and UI images by evaluating the different thresholds (−0.4, −02, and 0).

As can be seen in TABLE 1, the threshold −0.2 had the best performance for detecting the urban areas from the NDBI image while the threshold −0.4 had the best performance for detecting the urban areas from the UI image. The experiment results in TABLE 1 show that although both the NDBI and UI images can be utilized for detecting the urban areas, the most suitable thresholds for detecting the urban areas from the NDBI and UI images may be different. Both urban areas separately generated from the NDBI image by evaluating the threshold −0.2 and from the UI image by evaluating the threshold −0.4, however, had misclassification errors, where the bare soil areas were classified into urban areas or where the high−rise apartments were classified into other areas (see FIGURES 7 and 8).

2. Discussion

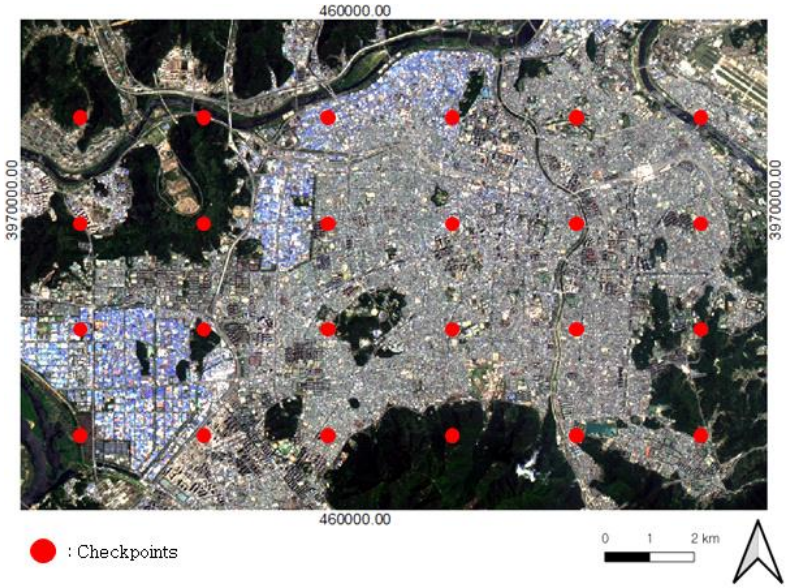

FIGURE 6. Checkpoints manually digitized based on the given Landsat−8 satellite image

TABLE 1. Accuracy of each urban map separately generated from the NDBI and UI images by evaluating the different thresholds (−0.4, −02, and 0): (a) Accuracy of the urban map generated from the NDBI image by evaluating the threshold -0.4; (b) Accuracy of the urban map generated from the NDBI image by evaluating the threshold -0.2; (c) Accuracy of the urban map generated from the NDBI image by evaluating the threshold 0; (d) Accuracy of the urban map generated from the UI image by evaluating the threshold -0.4; (e) Accuracy of the urban map generated from the UI image by evaluating the threshold -0.2; and (f) Accuracy of the urban map generated from the UI image by evaluating the threshold 0

(a)

Overall accuracy		68%	
Producer' s accuracy		User' s accuracy	
Urban area	100%	Urban area	63%
Other area	30%	Other area	100%

(b)

Overall accuracy		88%	
Producer' s accuracy		User' s accuracy	
Urban area	98%	Urban area	83%
Other area	76%	Other area	97%

(c)

Overall accuracy		66%	
Producer' s accuracy		User' s accuracy	
Urban area	41%	Urban area	92%
Other area	96%	Other area	58%

(d)

Overall accuracy		88%	
Producer' s accuracy		User' s accuracy	
Urban area	100%	Urban area	82%
Other area	74%	Other area	100%

(e)

Overall accuracy		80%	
Producer' s accuracy		User' s accuracy	
Urban area	70%	Urban area	90%
Other area	91%	Other area	72%

(f)

Overall accuracy		54%	
Producer' s accuracy		User' s accuracy	
Urban area	15%	Urban area	100%
Other area	100%	Other area	50%

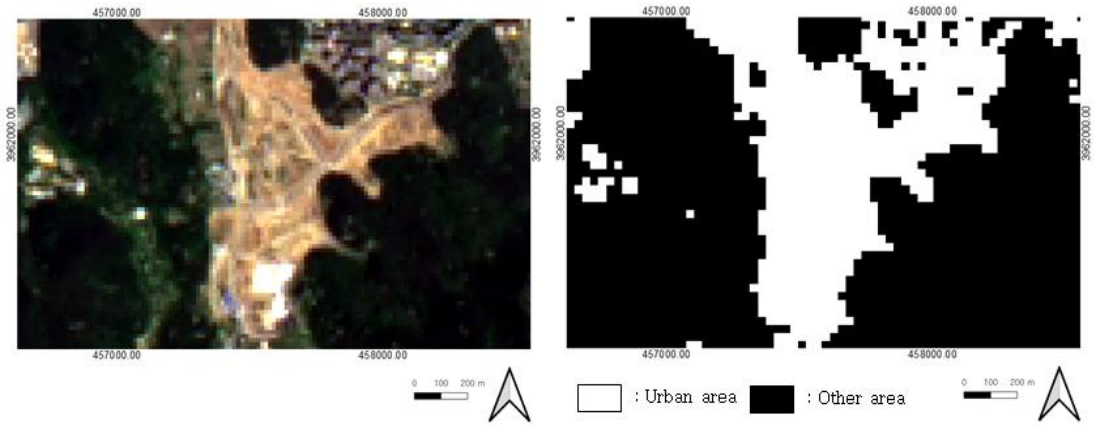

FIGURE 7. Example of the misclassification errors that occurred in the areas where the bare soil areas were classified into urban areas: (a) the given Landsat−8 image showing the bare soil areas; (b) the urban area detected from the NDBI image by evaluating the threshold -0.2; and (c) the urban area detected from the UI image by evaluating the threshold -0.4

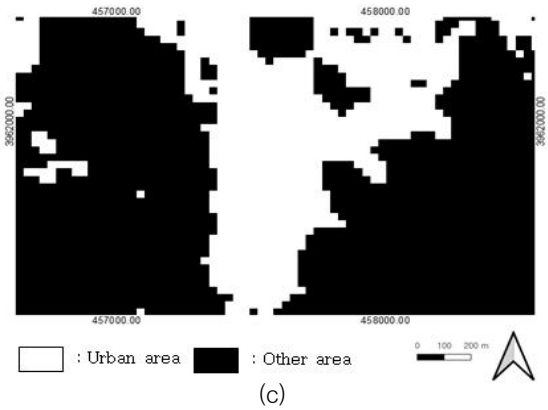

(c)

FIGURE 7. Continued

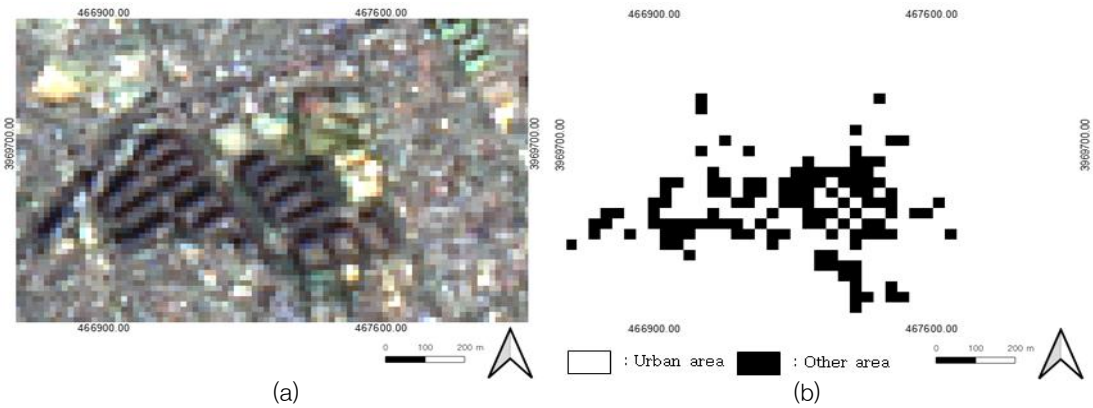

(a) (b)

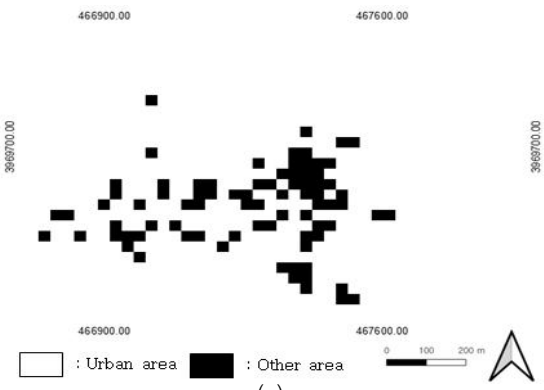

(c)

FIGURE 8. Example of the misclassification errors that occurred in the areas where the high-rise apartments were classified into other areas: (a) the given Landsat-8 image showing the high-rise apartments; (b) the urban area detected from the NDBI image by evaluating the threshold -0.2; and (c) the urban area detected from the UI image by evaluating the threshold -0.4

Conclusions

In this research, the different thresholds (−0.4, −0.2, 0) for detecting the urban areas separately from both the normalized−difference built−in index (NDBI) and urban index (UI) images were evaluated. The experiment results showed that the threshold −0.2 had the best performance for detecting the urban areas from the NDBI image while the threshold −0.4 had the best performance for detecting the urban areas from the UI image. Both results, however, had misclassification errors in some areas, where the bare soil areas were classified into urban areas and the high−rise apartments were classified into other areas. Hence, in the future research, a more robust methodology for detecting the various types of urban features from the earth observation satellite images will be proposed. In addition, research on analyzing the pattern of urban expansion will be carried out using the urban areas detected from the multi−temporal satellite images. KAGIS

REFERENCES

Bhatti, S. and N. Tripathi. 2014. Built−up area extraction using Landsat 8 OLI imagery. GIScience & Remote Sensing 51(4):445−467.

Choung, Y.J. and J.M. Kim. 2019. Study of the Relationship between Urban Expansion and PM_{10} Concentration Using Multi−Temporal Spatial Datasets and the Machine Learning Technique: Case Study for Daegu, South Korea. Applied Sciences 9(6):1098.

Corbane, C., J.F. Faure, N. Baghdadi, N. Villeneuve and M. Petit. 2008. Rapid Urban Mapping Using SAR/Optical Imagery Synergy. Sensors 8(11):7125−7143.

Han, R., P. Liu, H. Wang, L. Yang, H. Zhang and C. Ma. 2017. An Improved Urban Mapping Strategy Based on Collaborative Processing of Optical and SAR Remotely Sensed Data. Mathematical Problems in Engineering 2017:1−9.

Hu, T., J. Yang, X. Li and P. Gong. 2016. Mapping Urban Land Use by Using Landsat Images and Open Social Data. Remote Sensing 8(2):1−18.

Jensen, J.R. 2016. Introductory Digital Image Processing: A Remote Sensing Perspective (4th Edition). Pearson Series in Geographic Information Science. London, United Kingdom, 656 pp.

Kim, J.I., K.W. Hwang, H.W. Chung and C.H. Yeo. 2004. Urban Growth Analysis Through Satellite Image and Zonal Data. Journal of the Korean Association of Geographic Information Studies 7(3):1−12.

Kim, J.I. and J.H. Kwon. 2009. Identifying Urban Spatial Structure through GIS and Remote Sensing Data. Journal of the Korean Association of Geographic Information Studies 12(2):44−51.

Kim, Y.S., K.J. Lee, J.W. Ryu and J.H. Kim. 2003. Landuse Classification Nomenclature for Urban Growth Analysis Using Satellite Imagery. Journal of the Korean Association of Geographic Information Studies 6(3):83−94.

Li, H., C. Wang, C. Zhong, A. Su, C. Xiong, J. Wang and J. Liu. 2017a. Mapping Urban Bare Land Automatically from Landsat Imagery with a Simple Index. Remote Sensing 9(3): 1-15.

Li, H., C. Wang, C. Zhong, Z. Zhang and Q. Liu. 2017b. Mapping Typical Urban LULC from Landsat Imagery without Training Samples or Self-Defined Parameters. Remote Sensing 9(7): 1-23.

National Geographic. Urban area. https://www.nationalgeographic.org/encyclopedia/urban-area/ (assessed on March 25, 2019).

Sertel, E. and S. Akay. 2015. High resolution mapping of urban areas using SPOT-5 images and ancillary data. International Journal of Environment and Geoinformatics 2(2): 63-76.

United States Geological Survey (USGS). 2019. Landsat Missions. https://www.usgs.gov/land-resources/nli/landsat (assessed on March 25, 2019).